Numer. Math. Theor. Meth. Appl.
doi: 10.4208/nmtma.2017.m1617

Vol. **10**, No. 1, pp. 1-21
February 2017

Phaseless Imaging by Reverse Time Migration: Acoustic Waves

Zhiming Chen[1,*] and Guanghui Huang[2]

[1] *LSEC, Institute of Computational Mathematics, Academy of Mathematics and Systems Science, Chinese Academy of Sciences, Beijing 100190, China; School of Mathematical Sciences, University of Chinese Academy of Sciences, Beijing 100049, China*
[2] *The Rice Inversion Project, Department of Computational and Applied Mathematics, Rice University, Houston, TX 77005-1892, USA*

Received 19 April 2016; Accepted (in revised version) 5 May 2016

Abstract. We propose a reliable direct imaging method based on the reverse time migration for finding extended obstacles with phaseless total field data. We prove that the imaging resolution of the method is essentially the same as the imaging results using the scattering data with full phase information when the measurement is far away from the obstacle. The imaginary part of the cross-correlation imaging functional always peaks on the boundary of the obstacle. Numerical experiments are included to illustrate the powerful imaging quality.

AMS subject classifications: 78A46

Key words: Reverse time migration, phaseless data, inverse scattering, extended obstacle.

1. Introduction

We consider in this paper inverse scattering problems with phaseless data which aim to find the support of unknown obstacles from the knowledge of the amplitude of the total field measured on a given surface far away from the obstacles. Let the sound soft obstacle occupy a bounded Lipschitz domain $D \subset \mathbb{R}^2$ with ν the unit outer normal to its boundary Γ_D. Let u^i be the incident wave and the total field is $u = u^i + u^s$ with u^s being the solution of the following acoustic scattering problem:

$$\Delta u^s + k^2 u^s = 0 \quad \text{in } \mathbb{R}^2 \backslash \bar{D}, \tag{1.1}$$

$$u^s = -u^i \quad \text{on } \Gamma_D, \tag{1.2}$$

$$\sqrt{r}\Big(\frac{\partial u^s}{\partial r} - \mathbf{i}k u^s\Big) \to 0 \ \text{ as } \ r = |x| \to +\infty, \tag{1.3}$$

*Corresponding author. *Email addresses:* zmchen@lsec.cc.ac.cn (Z.-M. Chen), ghhuang@rice.edu (G.-H. Huang)

 ©2017 Global-Science Press

https://doi.org/10.4208/nmtma.2017.m1617 Published online by Cambridge University Press

where $k > 0$ is the wave number. The condition (1.3) is the outgoing Sommerfeld radiation condition which guarentees the uniqueness of the solution. In this paper, by the radiation or scattering solution we always mean the solution satisfies the Sommerfeld radiation condition (1.3). For the sake of the simplicity, we mainly consider the imaging of sound soft obstacles in this paper. The extension of our theoretical results for imaging other types of obstacles will be briefly considered in Section 4.

In the diffractive optics imaging and radar imaging systems, it is much easier to measure the intensity of the total field than the phase information of the field [11, 12, 36]. It is thus very desirable to develop reliable numerical methods for reconstructing obstacles with only phaseless data, that is, the amplitude information of the total field $|u|$. In recent years, there have been considerable efforts in the literature to solve the inverse scattering problems with phaseless data. One approach is to image the object with the phaseless data directly in the inversion algorithm, see e.g. [12, 24, 25]. The other approach is first to apply the phase retrieval algorithm to extract the phase information of the scattering field from the measurement of the intensity and then use the retrieved full field data in the classical imaging algorithms, see e.g. [13]. In [19, 20], explicit formulas are provided for the reconstruction by using Radon transform. Theoretical analysis of the phaseless inverse scattering problems and reconstruction procedures with the scattering amplitude are provided in [29, 30]. Resolution and stability analysis together with reconstruction procedures by phaseless data are obtained in [1] by using the concept of scattering coefficients based on the linearization method. We also refer to [2] for the continuation method and [16, 17, 22] for inverse scattering problems with the data of the amplitude of the far field pattern. In [18] some uniqueness results for phaseless inverse scattering problems have been obtained.

The reverse time migration (RTM) method, which consists of back-propagating the complex conjugated scattering field into the background medium and computing the cross-correlation between the incident wave field and the backpropagated field to output the final imaging profile, is nowadays a standard imaging technique widely used in seismic imaging [3]. Let $\Gamma_s = \partial B_s$ and $\Gamma_r = \partial B_r$, where B_s, B_r are the disks of radius R_s, R_r respectively. Without loss of generality, we assume $R_r \geq R_s$. We denote by Ω the sampling domain in which the obstacle is sought. Let $u^i(x, x_s) = \Phi(x, x_s)$, where $\Phi(x, x_s) = \frac{\mathrm{i}}{4} H_0^{(1)}(k|x - x_s|)$ is the fundamental solution of the Helmholtz equation with the source at $x_s \in \Gamma_s$, be the incident wave and $u^s(x, x_s)$ is the solution to the problem (1.1)-(1.3) with $u^i(x, x_s) = \Phi(x, x_s)$. The RTM imaging function studied in [4] for reconstructing extended targets is

$$I_{\mathrm{RTM}}(z) = -k^2 \mathrm{Im} \int_{\Gamma_s} \int_{\Gamma_r} \Phi(z, x_s) \Phi(x_r, z) \overline{u^s(x_r, x_s)} ds(x_r) ds(x_s), \quad \forall\, z \in \Omega, \tag{1.4}$$

where Ω is the sampling domain that the obstacle is sought. It is shown in [4] that this imaging function always peaks on the boundary of the obstacle. In [5, 6], the RTM methods for reconstructing extended targets using electromagnetic and elastic waves at a fixed frequency are proposed and studied.

https://doi.org/10.4208/nmtma.2017.m1617 Published online by Cambridge University Press

In this paper we propose the following imaging function based on reverse time migration for imaging obstacles with only intensity measurement $|u|$:

$$I_{\rm RTM}^{\rm phaseless}(z) = -k^2 {\rm Im} \int_{\Gamma_s} \int_{\Gamma_r} \Phi(z, x_s) \Phi(x_r, z) \Delta(x_r, x_s) ds(x_r) ds(x_s), \quad \forall\, z \in \Omega, \quad (1.5)$$

where

$$\Delta(x_r, x_s) = \frac{|u(x_r, x_s)|^2 - |u^i(x_r, x_s)|^2}{u^i(x_r, x_s)}. \quad (1.6)$$

We will show in Theorem 3.1 below that

$$I_{\rm RTM}^{\rm phaseless}(z) = I_{\rm RTM}(z) + O((kR_s)^{-1/2}).$$

Therefore the imaging resolution of our new phaseless RTM algorithm is essentially the same as the imaging results using the scattering data with the full phase information when the sources and measurements are placed far away from the scatterer. To the best knowledge of the authors, our method seems to be the first attempt in applying non-iterative method for reconstructing obstacles with phaseless data except [11] in which a direct method is considered for imaging a penetrable obstacle under Born approximation using plane wave incidences. We will extend the RTM method studied in this paper for electromagnetic probe waves in a future paper.

The rest of this paper is organized as follows. In Section 2 we introduce our RTM algorithm for imaging the obstacle with phaseless data. In Section 3 we consider the resolution of our algorithm for imaging sound soft obstacles. In Section 4 we extend our theoretical results to non-penetrable obstacles with the impedance boundary condition and penetrable obstacles. In Section 5 we report several numerical experiments to show the competitive performance of our phaseless RTM algorithm.

2. Reverse time migration method

In this section we introduce the RTM method for inverse scattering problems with phaseless data. Assume that there are N_s emitters and N_r receivers uniformly distributed respectively on Γ_s and Γ_r. We assume the obstacle $D \subset \Omega$ and Ω is inside B_s, B_r.

Let $u^i(x, x_s) = \Phi(x, x_s)$, where $\Phi(x, x_s) = \frac{\mathbf{i}}{4} H_0^{(1)}(k|x - x_s|)$ is the fundamental solution of the Helmholtz equation with the source at $x_s \in \Gamma_s$, be the incident wave and

$$|u(x_r, x_s)| = |u^s(x_r, x_s) + u^i(x_r, x_s)| \quad (2.1)$$

be the phaseless data received at $x_r \in \Gamma_r$, where $u^s(x, x_s)$ is the solution to the problem (1.1)-(1.3) with $u^i(x, x_s) = \Phi(x, x_s)$. We additionally assume that $x_s \neq x_r$ for all $s = 1, ..., N_s, r = 1, ..., N_r$, to avoid the singularity of the incident field $u^i(x, x_s)$ at $x = x_r$. This assumption can be easily satisfied in practical applications. In the following, without loss of generality, we assume $R_r = \tau R_s, \tau \geq 1$.

https://doi.org/10.4208/nmtma.2017.m1617 Published online by Cambridge University Press

Our RTM algorithm consists of back-propagating the corrected data $\Delta(x_r, x_s)$ in (1.6) into the domain using the fundamental solution $\Phi(x_r, z)$ and then computing the imaginary part of the cross-correlation between $u^i(z, x_s)$ and the back-propagated field.

Algorithm 2.1. *(RTM for Phaseless data) Given the data of* (2.1) *which is the measurement of the total field at $x_r \in \Gamma_r$ when the point source is emitted at $x_s \in \Gamma_s$, $s = 1, \ldots, N_s$, $r = 1, \ldots, N_r$.*

1. *Back-propagation: For $s = 1, \ldots, N_s$, compute the back-propagation field*

$$v_b(z, x_s) = -\frac{2\pi R_r}{N_r} \sum_{r=1}^{N_r} \Phi(x_r, z)\Delta(x_r, x_s), \quad \forall\, z \in \Omega. \tag{2.2}$$

2. *Cross-correlation: For $z \in \Omega$, compute*

$$I(z) = k^2 \mathrm{Im} \left\{ \frac{2\pi R_s}{N_s} \sum_{s=1}^{N_s} u^i(z, x_s) v_b(z, x_s) \right\}. \tag{2.3}$$

It is easy to see that

$$I(z) = -k^2 \mathrm{Im} \left\{ \frac{(2\pi)^2 R_s R_r}{N_s N_r} \sum_{s=1}^{N_s} \sum_{r=1}^{N_r} \Phi(z, x_s)\Phi(x_r, z)\Delta(x_r, x_s) \right\}, \quad \forall\, z \in \Omega. \tag{2.4}$$

This is the formula used in our numerical experiments in Section 4. By letting $N_s, N_r \to \infty$, we know that (2.4) can be viewed as an approximation of the continuous imaging function $I_{\mathrm{RTM}}^{\mathrm{phaseless}}$ in (1.5).

We remark that the above RTM imaging algorithm is the same as the RTM method in [4] except that the input data now is $\Delta(x_r, x_s)$ instead of $\overline{u^s(x_r, x_s)}$. Hence, the code of the RTM algorithm for imaging the obstacle with phaseless data requires only one line change from the code of the RTM method for imaging the obstacle with full phase information.

3. The resolution analysis

In this section we study the resolution of the Algorithm 2.1. We first introduce some notation. For any bounded domain $U \subset \mathbb{R}^2$ with Lipschitz boundary Γ, let

$$\|u\|_{H^1(U)} = (\|\nabla\phi\|^2_{L^2(U)} + d_U^{-2}\|\phi\|^2_{L^2(U)})^{1/2}$$

be the weighted $H^1(U)$ norm and

$$\|v\|_{H^{1/2}(\Gamma)} = (d_U^{-1}\|v\|^2_{L^2(\Gamma)} + |v|^2_{\frac{1}{2},\Gamma})^{1/2}$$

https://doi.org/10.4208/nmtma.2017.m1617 Published online by Cambridge University Press

be the weighted $H^{1/2}(\Gamma)$ norm, where d_U is the diameter of U and

$$|v|_{\frac{1}{2},\Gamma} = \left(\int_\Gamma \int_\Gamma \frac{|v(x) - v(y)|^2}{|x-y|^2} ds(x) ds(y) \right)^{1/2}.$$

By scaling argument and trace theorem we know that there exists a constant $C > 0$ independent of d_D such that for any $\phi \in C^1(\bar{D})$,

$$\|\phi\|_{H^{1/2}(\Gamma_D)} + \|\partial\phi/\partial\nu\|_{H^{-1/2}(\Gamma_D)} \le C \max_{x\in\bar{D}} \Big(|\phi(x)| + d_D |\nabla\phi(x)| \Big). \tag{3.1}$$

The following stability estimate of the forward acoustic scattering problem is well-known [10, 26].

Lemma 3.1. *Let $g \in H^{1/2}(\Gamma_D)$. Then the scattering problem:*

$$\Delta w + k^2 w = 0 \qquad \text{in } \mathbb{R}^2\backslash\bar{D}, \quad w = g \quad \text{on } \Gamma_D, \tag{3.2}$$

$$\sqrt{r}\left(\frac{\partial w}{\partial r} - \mathbf{i}kw \right) \to 0, \quad \text{as } r \to \infty, \tag{3.3}$$

admits a unique solution $w \in H^1_{\rm loc}(\mathbb{R}^2\backslash\bar{D})$. Moreover, there exists a constant $C > 0$ such that

$$\|\partial w/\partial\nu\|_{H^{-1/2}(\Gamma_D)} \le C \|g\|_{H^{1/2}(\Gamma_D)}.$$

We define $\mathbb{T} : H^{1/2}(\Gamma_D) \to H^{-1/2}(\Gamma_D)$ the Dirichlet-to-Neumann mapping for the scattering problem (3.2)-(3.3) as follows: for any $g \in H^{1/2}(\Gamma_D)$, $\mathbb{T}(g) = \frac{\partial w}{\partial \nu}$. By Lemma 3.1, $\mathbb{T}$ is a bounded linear operator and we will denote $\|\mathbb{T}\|$ its operator norm in this paper.

The far field pattern $w^\infty(\hat{x})$, where $\hat{x} = x/|x| \in S^1 = \{x \in \mathbb{R}^2 : |x| = 1\}$, of the solution of the scattering problem (3.2)-(3.3) is defined as (cf. e.g. [10, P. 67]):

$$w^\infty(\hat{x}) = \frac{e^{\mathbf{i}\frac{\pi}{4}}}{\sqrt{8\pi k}} \int_{\Gamma_D} \left[w(y) \frac{\partial e^{-\mathbf{i}k\hat{x}\cdot y}}{\partial\nu(y)} - \frac{\partial w(y)}{\partial\nu(y)} e^{-\mathbf{i}k\hat{x}\cdot y} \right] ds(y). \tag{3.4}$$

It is well-known that for the scattering solution of (3.2)-(3.3) (cf. e.g. [4, Lemma 3.3])

$$-\operatorname{Im} \int_{\Gamma_D} w \frac{\partial \bar{w}}{\partial\nu} ds = k \int_{S^1} |w^\infty(\hat{x})|^2 d\hat{x}. \tag{3.5}$$

Now we turn to the analysis of the imaging function $I^{\rm phaseless}_{\rm RTM}(z)$ in (1.5). We first observe that

$$\Delta(x_r, x_s) = \overline{u^s(x_r, x_s)} + \frac{|u^s(x_r, x_s)|^2}{u^i(x_r, x_s)} + \frac{u^s(x_r, x_s)\overline{u^i(x_r, x_s)}}{u^i(x_r, x_s)}. \tag{3.6}$$

This yields, for any $z \in \Omega$,

https://doi.org/10.4208/nmtma.2017.m1617 Published online by Cambridge University Press

$$
\begin{aligned}
&I_{\rm RTM}^{\rm phaseless}(z)\\
&= I_{\rm RTM}(z) - k^2 {\rm Im} \int_{\Gamma_s}\int_{\Gamma_r} \Phi(z,x_s)\Phi(x_r,z)\frac{|u^s(x_r,x_s)|^2}{u^i(x_r,x_s)}ds(x_r)ds(x_s)\\
&\quad -k^2 {\rm Im} \int_{\Gamma_s}\int_{\Gamma_r} \Phi(z,x_s)\Phi(x_r,z)\frac{u^s(x_r,x_s)\overline{u^i(x_r,x_s)}}{u^i(x_r,x_s)}ds(x_r)ds(x_s), \qquad (3.7)
\end{aligned}
$$

where $I_{\rm RTM}(z)$ is defined in (1.4). Our goal now is to show the last two terms at the right hand side of (3.7) are small when $kR_s \gg 1$. We start with the following lemma.

Lemma 3.2. *We have*

$$|u^s(x_r,x_s)| \le C(1+\|\mathbb{T}\|)(kR_r)^{-1/2}(kR_s)^{-1/2} \quad \forall x_r \in \Gamma_r, x_s \in \Gamma_s,$$

where the constant C may depend on kd_D but is independent of k, d_D, R_r, R_s.

Proof. We first recall the following estimates for Hankel functions [8, (1.22)-(1.23)]:

$$|H_0^{(1)}(t)| \le \left(\frac{2}{\pi t}\right)^{1/2}, \quad |H_1^{(1)}(t)| \le \left(\frac{2}{\pi t}\right)^{1/2} + \frac{2}{\pi t}, \quad \forall t>0. \qquad (3.8)$$

By the integral representation formula, we have

$$u^s(x_r,x_s) = \int_{\Gamma_D}\left(u^s(y,x_s)\frac{\partial\Phi(x_r,y)}{\partial\nu(y)} - \frac{\partial u^s(y,x_s)}{\partial\nu(y)}\Phi(x_r,y)\right)ds(y). \qquad (3.9)$$

By (3.1) we have

$$\|\Phi(x_r,\cdot)\|_{H^{1/2}(\Gamma_D)} + \|\partial\Phi(x_r,\cdot)/\partial\nu\|_{H^{-1/2}(\Gamma_D)} \le C(kR_r)^{-1/2}.$$

The lemma follows now from Lemma 3.1 and the fact that $u^i(y,x_s) = -\Phi(y,x_s)$ for $y \in \Gamma_D$. □

Lemma 3.3. *We have $|H_0^{(1)}(t)| \ge [2/(5\pi e)]|\ln t|$ for any $t \in (0,1)$.*

Proof. We use the following integral formula [8, 31]

$$H_0^{(1)}(t) = -\frac{2\mathbf{i}}{\pi}e^{\mathbf{i}t}\int_0^\infty \frac{e^{-rt}}{r^{1/2}(r-2\mathbf{i})^{1/2}}dr, \quad \forall t>0,$$

where ${\rm Re}\,(r-2\mathbf{i})^{1/2} > 0$ for $r>0$. By the change of variable

$$
\begin{aligned}
|H_0^{(1)}(t)| &\ge \frac{2}{\pi}{\rm Re}\int_0^\infty \frac{e^{-s}}{s^{1/2}(s-2\mathbf{i}t)^{1/2}}ds = \frac{2}{\pi}\int_0^\infty \frac{e^{-s}}{s^{1/2}|s-2\mathbf{i}t|}\sqrt{\frac{|s-2\mathbf{i}t|+s}{2}}ds\\
&\ge \frac{2}{\pi}\int_0^\infty \frac{e^{-s}}{|s-2\mathbf{i}t|}ds \ge \frac{2}{5\pi}\int_t^1 \frac{e^{-s}}{s}ds,
\end{aligned}
$$

https://doi.org/10.4208/nmtma.2017.m1617 Published online by Cambridge University Press

where in the last inequality we have used $|s - 2\mathbf{i}t| \le 5s$ for $s \ge t$. This completes the proof by noticing that $\int_t^1 s^{-1}e^{-s}ds \ge e^{-1}\int_t^1 s^{-1}ds = e^{-1}|\ln t|$. □

The following lemma gives an estimate of the second term at the right hand side of (3.7).

Lemma 3.4. *We have*

$$\left|k^2\int_{\Gamma_s}\int_{\Gamma_r}\Phi(z,x_s)\Phi(x_r,z)\frac{|u^s(x_r,x_s)|^2}{u^i(x_r,x_s)}ds(x_r)ds(x_s)\right| \le C(1+\|\mathbb{T}\|)^2(kR_s)^{-1/2},$$

where the constant C may depend on kd_D but is independent of k, d_D, R_r, R_s.

Proof. Denote $\Omega_k = \{(x_r,x_s)\in\Gamma_r\times\Gamma_s : |x_r - x_s| < 1/(2k)\}$. By (3.8) and Lemma 3.2,

$$\left|\iint_{\Omega_k}\Phi(z,x_s)\Phi(x_r,z)\frac{|u^s(x_r,x_s)|^2}{u^i(x_r,x_s)}ds(x_r)ds(x_s)\right| \le C(1+\|\mathbb{T}\|)^2(kR_s)^{-3/2}(kR_r)^{-3/2}\iint_{\Omega_k}\frac{1}{|\ln(k|x_r-x_s|)|}ds(x_r)ds(x_s). \quad (3.10)$$

Since $k|x_r - x_s| < 1/2$ for $x_r, x_s \in \Omega_k$, we have

$$\iint_{\Omega_k}\frac{1}{|\ln(k|x_r-x_s|)|}ds(x_r)ds(x_s) \le \frac{1}{\ln(2)}\iint_{\Omega_k}ds(x_r)ds(x_s) \le CR_rR_s,$$

Substituting the above estimate into (3.10) we obtain

$$\left|\iint_{\Omega_k}\Phi(z,x_s)\Phi(x_r,z)\frac{|u^s(x_r,x_s)|^2}{u^i(x_r,x_s)}ds(x_r)ds(x_s)\right| \le Ck^{-2}(1+\|\mathbb{T}\|)^2(kR_s)^{-1}. \quad (3.11)$$

Next we estimate the integral in $\Gamma_r\times\Gamma_s\backslash\bar{\Omega}_k$. Since $t|H_0^{(1)}(t)|^2$ is an increasing function of $t > 0$ [34, p. 446], we have for $(x_r,x_s)\in\Gamma_r\times\Gamma_s\backslash\bar{\Omega}_k$, $|x_r - x_s| \ge 1/(2k)$, and thus

$$|x_r - x_s||u^i(x_r,x_s)|^2 \ge \frac{1}{32}k^{-1}\left|H_0^{(1)}\left(\frac{1}{2}\right)\right|^2 = Ck^{-1},$$

which implies by using Lemma 3.2 and (3.8) again that

$$\left|\iint_{\Gamma_r\times\Gamma_s\backslash\bar{\Omega}_k}\Phi(z,x_s)\Phi(x_r,z)\frac{|u^s(x_r,x_s)|^2}{u^i(x_r,x_s)}ds(x_r)ds(x_s)\right| \le Ck^{-2}(1+\|\mathbb{T}\|)^2(kR_s)^{-1/2}. \quad (3.12)$$

https://doi.org/10.4208/nmtma.2017.m1617 Published online by Cambridge University Press

This completes the proof by combining the above estimate with (3.11). □

Now we turn to the estimation of the third term at the right hand side of (3.7). Denote $\delta = (kR_s)^{-1/2}$ and $\Theta_\delta := \{(\theta_r, \theta_s) \in (0, 2\pi)^2 : |\theta_r - \theta_s \pm m\pi| < \delta,\ m = 0, 1, 2\}$ and $Q_\delta := \{(x_r, x_s) \in \Gamma_r \times \Gamma_s : (\theta_r, \theta_s) \in \Theta_\delta\}$.

Lemma 3.5. *We have*

$$\left| k^2 \iint_{Q_\delta} \Phi(z, x_s)\Phi(x_r, z)u^s(x_r, x_s)\frac{\overline{u^i(x_r, x_s)}}{u^i(x_r, x_s)}ds(x_r)ds(x_s) \right| \leq C(1 + \|\mathbb{T}\|)(kR_s)^{-1/2},$$

where the constant C may depend on kd_D but is independent of k, d_D, R_r, R_s.

Proof. The proof follows easily from Lemma 3.2 and (3.8) and the fact that $|Q_\delta| \leq CR_rR_s(kR_s)^{-1/2}$. □

To estimate the integral in $\Gamma_r \times \Gamma_s \backslash \bar{Q}_\delta$, we recall first the following useful mixed reciprocity relation [21], [32, P.40].

Lemma 3.6. *Let $\gamma_m = e^{\mathbf{i}\frac{\pi}{4}}/\sqrt{8\pi k}$. Then $u^\infty_{\rm ps}(d, x_s) = \gamma_m u^s(x_s, -d)$ for any $x_s \in \mathbb{R}^2\backslash\bar{D}, d \in S^1$, where $u^\infty_{\rm ps}(d, x_s)$ is the far field pattern in the direction d of the scattering solution of* (1.1)-(1.3) *with $u^i(x) = \Phi(x, x_s)$ and $u^s(x, d)$ is the scattering solution of* (1.1)-(1.3) *with the incident plane wave $u^i(x) = e^{\mathbf{i}kx\cdot d}$.*

Lemma 3.7. *Let $u^\infty_{\rm pl}(\hat{x}_s, -\hat{x}_r)$ be the far field pattern in the direction $\hat{x}_s$ of the scattering solution of the Helmholtz equation with the incident plane wave $e^{-\mathbf{i}k\hat{x}_r\cdot x}$. Then $|u^\infty_{\rm pl}(\hat{x}_s, -\hat{x}_r)| + (kd_D)^{-1}|\partial u^\infty_{\rm pl}(\hat{x}_s, -\hat{x}_r)/\partial\theta_s| \leq Ck^{-1/2}(1 + \|\mathbb{T}\|)$, where the constant C may depend on kd_D but is independent of k, d_D.*

Proof. The proof follows from the definition of the far field pattern in (3.4) with $g(y) = -e^{-\mathbf{i}k\hat{x}_r\cdot y}$ on Γ_D, Lemma 3.1, and (3.1). Here we omit the details. □

The following lemma is essentially proved in [10, Theorem 2.5].

Lemma 3.8. *For any $x \in \mathbb{R}^2\backslash\bar{D}$, the solution of the scattering problem* (3.2)-(3.3) *satisfies the asymptotic behavior:*

$$w(x) = \frac{e^{\mathbf{i}k|x|}}{\sqrt{|x|}}w^\infty(\hat{x}) + \gamma(x),$$

where $|\gamma(x)| \leq C(1 + \|\mathbb{T}\|)(k|x|)^{-3/2}\|g\|_{H^{1/2}(\Gamma_D)}$, where the constant C may depend on kd_D but is independent of k, d_D.

Proof. First we have the following integral representation formula

$$w(x) = \int_{\Gamma_D} \left[w(y)\frac{\partial\Phi(x, y)}{\partial\nu(y)} - \Phi(x, y)\frac{\partial w(y)}{\partial\nu(y)} \right] ds(y), \quad \forall x \in \mathbb{R}^2\backslash\bar{D}. \tag{3.13}$$

https://doi.org/10.4208/nmtma.2017.m1617 Published online by Cambridge University Press

By the asymptotic formulae of Hankel functions [34, P.197], for $n = 1, 2$,

$$H_n^{(1)}(t) = \left(\frac{2}{\pi t}\right)^{1/2} e^{\mathbf{i}(kt - \frac{n\pi}{2} - \frac{\pi}{4})} + R_n(t), \quad |R_n(t)| \le Ct^{-3/2}, \quad \forall t > 0, \tag{3.14}$$

and the simple estimate $|k|x - y| - k(|x| - \hat{x} \cdot y)| \le C(k|y|)^2(k|x|)^{-1}$ for any $y \in \Gamma_D$, $x \in \mathbb{R}^2 \backslash \bar{D}$, we have

$$\Phi(x, y) = \frac{e^{\mathbf{i}\frac{\pi}{4}}}{\sqrt{8\pi k}} \frac{e^{\mathbf{i}k|x|}}{\sqrt{|x|}} e^{-\mathbf{i}k\hat{x}\cdot y} + \gamma_0(x, y), \tag{3.15}$$

$$\frac{\partial \Phi(x, y)}{\partial \nu(y)} = \frac{e^{\mathbf{i}\frac{\pi}{4}}}{\sqrt{8\pi k}} \frac{e^{\mathbf{i}k|x|}}{\sqrt{|x|}} \frac{\partial e^{-\mathbf{i}k\hat{x}\cdot y}}{\partial \nu(y)} + \gamma_1(x, y), \tag{3.16}$$

where $|\gamma_0(x, y)| + k^{-1}|\gamma_1(x, y)| \le C(1 + k|y|)^2(k|x|)^{-3/2}$ for some constant C independent of k and D. The proof completes by inserting (3.15)-(3.16) into (3.13) and using Lemma 3.1 and (3.1). Here we omit the details. □

We also need the following slight generalization of Van der Corput lemma for the oscillatory integral [14, P.152].

Lemma 3.9. *For any $-\infty < a < b < \infty$, for every real-valued C^2 function u that satisfies $|u'(t)| \ge 1$ for $t \in (a, b)$. Assume that $a = x_0 < x_1 < \cdots < x_N = b$ is a division of (a, b) such that u' is monotone in each interval (x_{i-1}, x_i), $i = 1, \cdots, N$. Then for any function ϕ defined on (a, b) with integrable derivative, and for any $\lambda > 0$,*

$$\left| \int_a^b e^{\mathbf{i}\lambda u(t)} \phi(t) dt \right| \le (2N + 2)\lambda^{-1} \left[|\phi(b)| + \int_a^b |\phi'(t)| dt \right].$$

Proof. By integration by parts we have

$$\int_a^b e^{\mathbf{i}\lambda u(t)} dt = \left[\frac{e^{\mathbf{i}\lambda u(t)}}{\mathbf{i}\lambda u'(t)} \right]_a^b - \int_a^b e^{\mathbf{i}\lambda u(t)} \frac{d}{dt} \left(\frac{1}{\mathbf{i}\lambda u'(t)} \right) dt.$$

Since u' is monotone in each interval (x_{i-1}, x_i), $i = 1, \cdots, N$, and $|u'(t)| \ge 1$ in (a, b), we have

$$\left| \int_a^b e^{\mathbf{i}\lambda u(t)} \frac{d}{dt} \left(\frac{1}{\mathbf{i}\lambda u'(t)} \right) dt \right| \le \sum_{i=1}^N \lambda^{-1} \left| \int_{x_{i-1}}^{x_i} \frac{d}{dt} \left(\frac{1}{u'(t)} \right) dt \right| \le 2N\lambda^{-1},$$

which implies $| \int_a^b e^{\mathbf{i}\lambda u(t)} dt| \le (2N + 2)\lambda^{-1}$. For the general case, we denote $F(t) = \int_a^t e^{\mathbf{i}\lambda u(s)} ds$ and use integration by parts to obtain

$$\int_a^b \phi(t) e^{\mathbf{i}\lambda u(t)} dt = \phi(b)F(b) - \int_a^b F(t)\phi'(t) dt.$$

This completes the proof by using $|F(t)| \le (2N + 2)\lambda^{-1}$. □

https://doi.org/10.4208/nmtma.2017.m1617 Published online by Cambridge University Press

Lemma 3.10. *We have*

$$\left| k^2 \iint_{\Gamma_r\times\Gamma_s\setminus\bar{Q}_\delta} \Phi(z,x_s)\Phi(x_r,z)u^s(x_r,x_s)\frac{\overline{u^i(x_r,x_s)}}{u^i(x_r,x_s)}ds(x_r)ds(x_s)\right| \leq C(1+\|\mathbb{T}\|)(kR_s)^{-1/2},$$

where the constant C may depend on $kd_D, k|z|$ but is independent of k, d_D, R_r, R_s.

Proof. We first observe that for $(x_r,x_s)\in\Gamma_r\times\Gamma_s\setminus\bar{Q}_\delta$, we have

$$k|x_r-x_s| \geq 2kR_s\sqrt{\tau}\left|\sin\frac{\theta_r-\theta_s}{2}\right| \geq 2kR_s\sqrt{\tau}\sin\frac{\delta}{2} \geq \frac{1}{2}(kR_s)^{1/2}\sqrt{\tau},$$

where we have used the fact that $\sin t \geq t/2$ for $t\in(0,\pi/2)$. Thus by (3.14) we obtain

$$\frac{\overline{u^i(x_r,x_s)}}{u^i(x_r,x_s)} = e^{-2\mathbf{i}k|x_r-x_s|+\mathbf{i}\frac{\pi}{2}} + \rho_0(x_r,x_s), \tag{3.17}$$

where $|\rho_0(x_r,x_s)|\leq C(kR_s)^{-1/2}$. Similar to (3.15) we have

$$\Phi(z,x_s) = \frac{e^{\mathbf{i}\frac{\pi}{4}}}{\sqrt{8\pi k}}\frac{e^{\mathbf{i}kR_s}}{\sqrt{R_s}}e^{-\mathbf{i}k\hat{x}_s\cdot z} + \rho_1(z,x_s), \tag{3.18}$$

$$\Phi(z,x_r) = \frac{e^{\mathbf{i}\frac{\pi}{4}}}{\sqrt{8\pi k}}\frac{e^{\mathbf{i}kR_r}}{\sqrt{R_r}}e^{-\mathbf{i}k\hat{x}_r\cdot z} + \rho_1(z,x_r), \tag{3.19}$$

where $|\rho_1(z,x_s)|\leq C(kR_s)^{-3/2}$, $|\rho_1(z,x_r)|\leq C(kR_r)^{-3/2}$. Next by Lemma 3.8, the mixed reciprocity in Lemma 3.6, and (3.1) we have

$$\begin{aligned} u^s(x_r,x_s) &= \frac{e^{\mathbf{i}kR_r}}{\sqrt{R_r}}u^\infty_{\mathrm{ps}}(\hat{x}_r,x_s) + \rho_2(x_r,x_s)\\ &= \frac{e^{\mathbf{i}kR_r}}{\sqrt{R_r}}\gamma_m u^s(x_s,-\hat{x}_r) + \rho_2(x_r,x_s)\\ &= \frac{e^{\mathbf{i}k(R_r+R_s)}}{\sqrt{R_rR_s}}\gamma_m u^\infty_{\mathrm{pl}}(\hat{x}_s,-\hat{x}_r) + \rho_2(x_r,x_s) + \rho_3(x_r,x_s), \end{aligned} \tag{3.20}$$

where $u^\infty_{\mathrm{pl}}(\hat{x}_s,-\hat{x}_r)$ is the far field pattern of the scattering solution of the Helmholtz equation with the incident plane wave $u^i = e^{-\mathbf{i}k\hat{x}_r\cdot x}$ and

$$\begin{aligned} |\rho_2(x_r,x_s)| &\leq C(1+\|\mathbb{T}\|)(kR_r)^{-3/2}\|\Phi(\cdot,x_s)\|_{H^{1/2}(\Gamma_D)}\\ &\leq C(1+\|\mathbb{T}\|)(kR_r)^{-3/2}(kR_s)^{-1/2},\\ |\rho_3(x_r,x_s)| &\leq C(1+\|\mathbb{T}\|)(kR_r)^{-1/2}(kR_s)^{-3/2}\|e^{-\mathbf{i}k\hat{x}_r\cdot x}\|_{H^{1/2}(\Gamma_D)}\\ &\leq C(1+\|\mathbb{T}\|)(kR_r)^{-1/2}(kR_s)^{-3/2}. \end{aligned}$$

https://doi.org/10.4208/nmtma.2017.m1617 Published online by Cambridge University Press

Combining (3.17)-(3.20) we have

$$k^2 \iint_{\Gamma_r\times\Gamma_s\setminus\bar{Q}_\delta} \Phi(z,x_s)\Phi(x_r,z)u^s(x_r,x_s)\frac{\overline{u^i(x_r,x_s)}}{u^i(x_r,x_s)}ds(x_r)ds(x_s)$$

$$= k^2R_sR_s \iint_{(0,2\pi)^2\setminus\bar{\Theta}_\delta} \Phi(z,x_s)\Phi(x_r,z)u^s(x_r,x_s)\frac{\overline{u^i(x_r,x_s)}}{u^i(x_r,x_s)}d\theta_r d\theta_s$$

$$= -\frac{\gamma_m k}{8\pi}e^{2\mathbf{i}k(R_r+R_s)} \iint_{(0,2\pi)^2\setminus\bar{\Theta}_\delta} \phi(\theta_r,\theta_s)e^{-2\mathbf{i}k|x_r-x_s|}d\theta_r d\theta_s + \rho(z), \qquad (3.21)$$

where $\phi(\theta_r,\theta_s) = u^\infty_{\rm pl}(\hat{x}_s,-\hat{x}_r)e^{-\mathbf{i}k(x_s+x_r)\cdot z}$ and by Lemma 3.2, $|\rho(z)| \le C(1+\|\mathbb{T}\|)(kR_s)^{-1/2}$.

Now direct calculation shows that

$$\begin{aligned}
&\iint_{(0,2\pi)^2\setminus\bar{\Theta}_\delta} \phi(\theta_r,\theta_s)e^{-2\mathbf{i}k|x_r-x_s|}d\theta_r d\theta_s\\
&= \int_0^\delta \int_{(\theta_r+\delta,\theta_r+\pi-\delta)\cup(\theta_r+\pi+\delta,\theta_r+2\pi-\delta)} \phi(\theta_r,\theta_s)e^{-2\mathbf{i}k|x_r-x_s|}d\theta_s d\theta_r\\
&\quad + \int_\delta^{\pi-\delta} \int_{(0,\theta_r-\delta)\cup(\theta_r+\delta,\theta_r+\pi-\delta)\cup(\theta_r+\pi+\delta,2\pi)} \phi(\theta_r,\theta_s)e^{-2\mathbf{i}k|x_r-x_s|}d\theta_s d\theta_r\\
&\quad + \int_{\pi-\delta}^{\pi+\delta} \int_{(\theta_r-\pi+\delta,\theta_r-\delta)\cup(\theta_r+\delta,\theta_r+\pi-\delta)} \phi(\theta_r,\theta_s)e^{-2\mathbf{i}k|x_r-x_s|}d\theta_s d\theta_r\\
&\quad + \int_{\pi+\delta}^{2\pi-\delta} \int_{(0,\theta_r-\pi-\delta)\cup(\theta_r-\pi+\delta,\theta_r-\delta)\cup(\theta_r+\delta,2\pi)} \phi(\theta_r,\theta_s)e^{-2\mathbf{i}k|x_r-x_s|}d\theta_s d\theta_r\\
&\quad + \int_{2\pi-\delta}^{2\pi} \int_{(\theta_r-2\pi+\delta,\theta_r-\pi-\delta)\cup(\theta_r-\pi+\delta,\theta_r-\delta)} \phi(\theta_r,\theta_s)e^{-2\mathbf{i}k|x_r-x_s|}d\theta_s d\theta_r\\
&=: \mathrm{I}_1+\cdots+\mathrm{I}_5. \qquad (3.22)
\end{aligned}$$

By Lemma 3.7 and $\delta = (kR_s)^{-1/2}$ we have $|\mathrm{I}_1+\mathrm{I}_3+\mathrm{I}_5| \le Ck^{-1/2}(1+\|\mathbb{T}\|)(kR_s)^{-1/2}$.

We will use Lemma 3.9 to estimate I_2 and I_4. For that purpose, denote by

$$v(\theta_s) = -\sqrt{1+\tau^2-2\tau\cos(\theta_r-\theta_s)}.$$

We have $v'(\theta_s) = \tau\sin(\theta_s-\theta_r)/v(\theta_s)$ and thus

$$|v'(\theta_s)| \ge \tau|\sin\delta|/|v(\theta_s)| \ge \frac{\tau}{1+\tau}\frac{\delta}{2} \ge \delta/4 = \frac{1}{4}(kR_s)^{-1/2}$$

for $(\theta_r,\theta_s)\in\Gamma_r\times\Gamma_s\setminus\bar{\Theta}_\delta$. Moreover,

$$v''(\theta_s) = -\tau^2(\cos(\theta_s-\theta_r)-\tau)(\cos(\theta_s-\theta_r)-\tau^{-1})/v(\theta_s)^3,$$

https://doi.org/10.4208/nmtma.2017.m1617 Published online by Cambridge University Press

which implies $v'(\theta_s)$ is piecewise monotone in $(0, 2\pi)$ for any fixed $\theta_r \in (0, 2\pi)$ since $\tau \geq 1$.

Now since $-2\mathbf{i}k|x_r - x_s| = 2\mathbf{i}kR_s v(\theta_s)$, we obtain by Lemma 3.9 and Lemma 3.7 that for $\theta_r \in (\delta, \pi - \delta)$,

$$\left| \int_0^{\theta_r - \delta} \phi(\theta_r, \theta_s) e^{-2\mathbf{i}k|x_r - x_s|} d\theta_s \right| \leq Ck^{-1/2}(1 + \|\mathbb{T}\|)(kR_s)^{-1/2}.$$

The other integrals in I_2 and I_4 can be estimated similarly to obtain

$$|\mathrm{I}_2| + |\mathrm{I}_4| \leq Ck^{-1/2}(1 + \|\mathbb{T}\|)(kR_s)^{-1/2}.$$

This completes the proof by (3.21). □

The following theorem is the main result of this section.

Theorem 3.1. *If the measured field* $|u(x_r, x_s)| = |u^s(x_r, x_s) + u^i(x_r, x_s)|$ *with* $u^s(x, x_s)$ *satisfying the problem* (1.1)-(1.3) *with the incident field* $u^i(x, x_s) = \Phi(x, x_s)$*, we have*

$$I_{\mathrm{RTM}}^{\mathrm{phaseless}}(z) = I_{\mathrm{RTM}}(z) + R_{\mathrm{RTM}}^{\mathrm{phaseless}}(z), \quad \forall z \in \Omega,$$

where $|R_{\mathrm{RTM}}^{\mathrm{phaseless}}(z)| \leq C(1 + \|\mathbb{T}\|)^2(kR_s)^{-1/2}$*. Here the constant* C *may depend on* $kd_D, k|z|$ *but is independent of* k, d_D, R_r, R_s*.*

Proof. The proof follows from (3.7), Lemma 3.5, and Lemma 3.10. □

For any $z \in \Omega$, let $\psi(x, z)$ be the scattering solution to the problem:

$$\Delta\psi(x, z) + k^2\psi(x, z) = 0 \quad \text{in } \mathbb{R}^2 \backslash \bar{D}, \quad \psi(x, z) = -\mathrm{Im}\,\Phi(x, z) \ \text{ on } \Gamma_D. \tag{3.23}$$

It is shown in [4, Theorem 3.2] that

$$I_{\mathrm{RTM}}(z) = k \int_{S^1} |\psi^\infty(\hat{x}, z)|^2 d\hat{x} + R_{\mathrm{RTM}}(z), \quad \forall z \in \Omega, \tag{3.24}$$

where $|R_{\mathrm{RTM}}(z)| \leq C(kR_s)^{-1}$. Since $\mathrm{Im}\,\Phi(x, z) = \frac{1}{4}J_0(k|x - z|)$ and it is well-known that $J_0(t)$ peaks at $t = 0$ and decays like $t^{-1/2}$ away from the origin, the source of the problem (3.23) will peak at the boundary of the scatterer D and becomes small when z moves away from ∂D. Thus the imaging function I_{RTM} and consequently $I_{\mathrm{RTM}}^{\mathrm{phaseless}}$ by Theorem 3.1 will have a large contrast at the boundary of the scatterer D and decay outside the boundary ∂D if $kR_s \gg 1$. This is indeed observed in our numerical experiments.

In the remainder of this section, we consider the physical interpretation of the imaging function $I_{\mathrm{RTM}}(z)$ for $z \in \Gamma_D$ in the high frequency limit $k \gg 1$. It indicates that $I_{\mathrm{RTM}}(z)$, and thus $I_{\mathrm{RTM}}^{\mathrm{phaseless}}(z)$ when $R_s \gg 1$ by Theorem 3.1, is of order one and inversely proportional to the curvature $\kappa(z)$ at the boundary point z. We first introduce the concept of the scattering coefficient for plane wave incidences, which is firstly proposed in [7] for analyzing the imaging functional defined in the half space.

https://doi.org/10.4208/nmtma.2017.m1617 Published online by Cambridge University Press

Definition 3.1. *For any unit vector $\eta \in \mathbb{R}^2$, let $v^i = e^{\mathbf{i}kx\cdot\eta}$ be the incident wave and v^s be the radiation solution of the Helmholtz equation:*

$$\Delta v^s + k^2 v^s = 0 \ \text{ in } \mathbb{R}^2\backslash\bar{D}, \quad v^s = -e^{\mathbf{i}kx\cdot\eta} \ \text{ on } \Gamma_D.$$

The scattering coefficient $R(x,\eta)$ for $x \in \Gamma_D$ is defined by the relation

$$\frac{\partial(v^s + v^i)}{\partial\nu} = \mathbf{i}kR(x,\eta)e^{\mathbf{i}kx\cdot\eta} \quad \text{on } \Gamma_D.$$

It is clear that the scattering coefficient $R(x,\eta)$ is well defined by the uniqueness and existence of the solution of Helmholtz scattering problems. The scattering coefficient is closely related to the concept of reflection coefficients that are widely used in the geophysics literature in different context based on geometric optics approximations.

For any $\xi \in \mathbb{R}^2\backslash\bar{D}$ far away from the scatterer, by the well-known asymptotic formula for the Hankel function we have

$$\begin{aligned}\Phi(x,\xi) &= \frac{\mathbf{i}}{4}\left(\frac{2}{k\pi|x-\xi|}\right)^{1/2} e^{\mathbf{i}k|x-\xi|-\mathbf{i}\frac{\pi}{4}} + O((k|\xi|)^{-3/2}) \\ &= \frac{e^{\mathbf{i}\frac{\pi}{4}}}{(8k\pi)^{1/2}}\frac{e^{\mathbf{i}k|\xi|}}{|\xi|^{1/2}}e^{-\mathbf{i}k\hat{\xi}\cdot x} + O((k|\xi|)^{-3/2}), \quad \forall x \in \Gamma_D.\end{aligned}$$

Let $G(x,\xi)$ be the Green function which satisfies

$$\begin{aligned}&\Delta G(x,\xi) + k^2 G(x,\xi) = -\delta_\xi(x) \quad \text{in } \mathbb{R}^2\backslash D, \\ &G(x,\xi) = 0 \quad \text{on } \Gamma_D, \\ &\sqrt{r}\left(\frac{\partial G(x,\xi)}{\partial r} - \mathbf{i}kG(x,\xi)\right) \to 0 \quad \text{as } r = |x| \to \infty,\end{aligned}$$

we know from the definition of the scattering coefficient that

$$\begin{aligned}\frac{\partial G(x,\xi)}{\partial\nu(x)} &= \mathbf{i}kR(x,-\hat{\xi})\frac{e^{\mathbf{i}\frac{\pi}{4}}}{(8k\pi)^{1/2}}\frac{e^{\mathbf{i}k|\xi|}}{|\xi|^{1/2}}e^{-\mathbf{i}k\hat{\xi}\cdot x} + O((k|\xi|)^{-3/2}) \\ &=: a(x,\hat{\xi})\frac{e^{\mathbf{i}k|\xi|}}{|\xi|^{1/2}}e^{-\mathbf{i}k\hat{\xi}\cdot x} + O((k|\xi|)^{-3/2}).\end{aligned}$$

Thus by integral representation we know that the solution of (3.23) satisfies

$$\begin{aligned}\psi(\xi,z) &= \int_{\Gamma_D}\psi(x,z)\frac{\partial G(x,\xi)}{\partial\nu(x)}ds(x) \\ &= \frac{e^{\mathbf{i}k|\xi|}}{|\xi|^{1/2}}\int_{\Gamma_D}\psi(x,z)a(x,\hat{\xi})e^{-ik\hat{\xi}\cdot x}ds(x) + O((k|\xi|)^{-3/2}).\end{aligned}$$

https://doi.org/10.4208/nmtma.2017.m1617 Published online by Cambridge University Press

In the case of Kirchhoff approximation when $k \gg 1$, see e.g. [3] and the mathematical justification for strictly convex obstacles in [27], the scattering coefficient can be approximated by

$$R(x,\eta) \approx \begin{cases} 2\nu(x)\cdot\eta & \text{if } x \in \partial D_\eta^- := \{x \in \Gamma_D : \nu(x)\cdot\eta < 0\}, \\ 0 & \text{if } x \in \partial D_\eta^+ := \{x \in \Gamma_D : \nu(x)\cdot\eta > 0\}. \end{cases}$$

Here ∂D_η^- and ∂D_η^+ are respectively the illuminating and shadow region for the incident wave $e^{\mathbf{i}kx\cdot\eta}$. This implies that

$$\psi^\infty(\hat{\xi}, z) \approx \int_{\partial D_{\hat{\xi}}^+} \psi(x,z) a(x,\hat{\xi}) e^{-\mathbf{i}k\hat{\xi}\cdot x} ds(x).$$

Now we are going to apply the following theorem of stationary phase, see e.g. [15, Theorem 7.7.5].

Lemma 3.11. *Let $g \in C_0^2(\mathbb{R})$ and the phase function $f \in C^2(\mathbb{R})$ has a stationary point at t_0 such that $f'(t_0) = 0$, $f''(t_0) \neq 0$, and $f'(t) \neq 0$ for $t \neq t_0$. Then for any $\lambda > 0$, there is a constant C such that*

$$\left| \int_{\mathbb{R}} g(t) e^{\mathbf{i}\lambda f(t)} dt - g(t_0) e^{\mathbf{i}\lambda f(t_0)} \left(\frac{\lambda f''(t_0)}{2\pi\mathbf{i}} \right)^{-1/2} \right| \leq C\lambda^{-1} \|g''\|_{C(\mathbb{R})}.$$

Let $x(s)$ be the arc length parametrization of the boundary Γ_D, $s \in (0, L)$. The phase function $f(s) = -\hat{\xi}\cdot x(s)$ satisfies $f'(s) = -\hat{\xi}\cdot x'(s), f''(s) = -\hat{\xi}\cdot x''(s)$. Let $x(\hat{\xi}) = x(s_0)$ be the point in $\partial D_{\hat{\xi}}^+$ such that $\nu(x(\hat{\xi}))$ is parallel to $\hat{\xi}$. Clearly we have $f'(s_0) = -\nu(x(\hat{\xi}))\cdot x'(s_0), f''(s_0) = -\nu(x(\hat{\xi}))\cdot x''(s_0) = -\kappa(x(\hat{\xi}))|x'(s_0)|^2$, where κ is the curvature of Γ_D. By Lemma 3.11 we have

$$\begin{aligned} \psi^\infty(\hat{\xi}, z) &= \psi(x(\hat{\xi}), z) a(x(\hat{\xi}), \hat{\xi}) e^{-\mathbf{i}k\hat{\xi}\cdot x(\hat{\xi})} \left(\frac{-k\kappa(x(\hat{\xi}))}{2\pi\mathbf{i}} \right)^{-1/2} + O(k^{-1}) \\ &= \psi(x(\hat{\xi}), z) \frac{-\mathbf{i}\, e^{-\mathbf{i}k\hat{\xi}\cdot x(\hat{\xi})}}{\sqrt{\kappa(x(\hat{\xi}))}} + O(k^{-1}). \end{aligned}$$

Therefore, by (3.24)

$$I_{\mathrm{RTM}}(z) \approx k \int_{S^1} \frac{|\operatorname{Im} \Phi(x(\hat{\xi}), z)|^2}{\kappa(x(\hat{\xi}))} d\hat{\xi}.$$

By the property of the Bessel function $J_0(k|x-z|)$, we know that the imaging function $I_{\mathrm{RTM}}(z)$ is inversely proportional to the curvature $\kappa(z)$ at z.

https://doi.org/10.4208/nmtma.2017.m1617 Published online by Cambridge University Press

4. Extensions

In this section we consider briefly the imaging of the penetrable and impedance non-penetrable obstacles with phaseless data. We first consider the imaging of impedance non-penetrable obstacles with the phaseless data, in which case, the measured phaseless total field $|u(x_r, x_s)| = |u^s(x_r, x_s) + u^i(x_r, x_s)|$, where $u^s(x, x_s)$ is the radiation solution of the following problem:

$$\Delta u^s + k^2 u^s = 0 \qquad \text{in } \mathbb{R}^2 \backslash \bar{D}, \tag{4.1}$$

$$\frac{\partial u^s}{\partial \nu} + \mathbf{i}k\eta(x)u^s = -\frac{\partial u^i}{\partial \nu} - \mathbf{i}k\eta(x)u^i \qquad \text{on } \Gamma_D. \tag{4.2}$$

Here $\eta(x) > 0$ is the impedance function. The well-posedness of the problem (4.1)-(4.2) is well-known [9, 23]. By modifying the argument in Section 3 we can show the following theorem whose proof is omitted.

Theorem 4.1. *If the measured field* $|u(x_r, x_s)| = |u^s(x_r, x_s) + u^i(x_r, x_s)|$ *with* $u^s(x, x_s)$ *satisfying* (4.1)-(4.2)*, we have, for any* $z \in \Omega$*,*

$$I_{\mathrm{RTM}}^{\mathrm{phaseless}}(z) = I_{\mathrm{RTM}}(z) + R_{\mathrm{RTM}}^{\mathrm{phaseless}}(z), \quad \forall z \in \Omega,$$

where $|R_{\mathrm{RTM}}^{\mathrm{phaseless}}(z)| \leq C(1 + \|\mathbb{T}\|)^2 (kR_s)^{-1/2}$*. Here the constant* C *may depend on* $kd_D, k|z|$ *but is independent of* k, d_D, R_r, R_s*.*

For penetrable obstacles, the measured total field $|u(x_r, x_s)| = |u^s(x_r, x_s) + u^i(x_r, x_s)|$, where $u^s(x, x_s)$ is the radiation solution of the following problem

$$\Delta u^s + k^2 n(x) u^s = -k^2 (n(x) - 1) u^i(x, x_s) \ \text{ in } \mathbb{R}^2 \tag{4.3}$$

with $n(x) \in L^\infty(\mathbb{R}^2)$ being a positive function which is equal to 1 outside the scatterer D. The well-posedness of the problem under some condition on $n(x)$ is known [35]. We can prove the following theorem by modifying the argument in Section 3. Here we omit the details.

Theorem 4.2. *If the measured field* $|u(x_r, x_s)| = |u^s(x_r, x_s) + u^i(x_r, x_s)|$ *with* $u^s(x, x_s)$ *satisfying* (4.3)*, we have*

$$I_{\mathrm{RTM}}^{\mathrm{phaseless}}(z) = I_{\mathrm{RTM}}(z) + R_{\mathrm{RTM}}^{\mathrm{phaseless}}(z), \quad \forall z \in \Omega,$$

where $|R_{\mathrm{RTM}}^{\mathrm{phaseless}}(z)| \leq C(1 + \|\mathbb{T}\|)^2 (kR_s)^{-1/2}$*. Here the constant* C *may depend on* $kd_D, k|z|$ *but is independent of* k, d_D, R_r, R_s*.*

We remark that for the impedance non-penetrable or penetrable scatterers, the studies in [4] show that the imaging function I_{RTM} will peak at the boundary of the scatterer if $R_s \gg 1$. Therefore we again expect the imaging function $I_{\mathrm{RTM}}^{\mathrm{phaseless}}(z)$ will have contrast on the boundary of the scatterer and decay outside the scatterer also for imaging impedance non-penetrable or penetrable scatterers.

https://doi.org/10.4208/nmtma.2017.m1617 Published online by Cambridge University Press

5. Numerical examples

In this section, we show several numerical experiments to illustrate the effectiveness of our RTM algorithm with phaseless data in this paper. To synthesize the scattering data we compute the solution $u(x, x_s)$ of the scattering problem (1.1)-(1.3) by standard Nyström's methods [10]. The boundary integral equations on Γ_D are solved on a uniform mesh over the boundary with ten points per probe wavelength. The boundaries of the obstacles used in our numerical experiments are parameterized as follows, where $\theta \in [0, 2\pi]$,

$$\begin{aligned}
\text{Circle:} \quad & x_1 = \rho\cos(\theta), \quad x_2 = \rho\sin(\theta), \\
\text{Kite:} \quad & x_1 = \cos(\theta) + 0.65\cos(2\theta) - 0.65, \quad x_2 = 1.5\sin(\theta), \\
p\text{-leaf:} \quad & r(\theta) = 1 + 0.2\cos(p\theta), \\
\text{Peanut:} \quad & x_1 = \cos(\theta) + 0.2\cos(3\theta), \quad x_2 = \sin(\theta) + 0.2\sin(3\theta), \\
\text{Rounded-square:} \quad & x_1 = \cos^3(\theta) + \cos(\theta), \quad x_2 = \sin^3(\theta) + \sin(\theta).
\end{aligned}$$

The sources x_s, $s = 1, \cdots, N_s$, and the receivers x_r, $x_r = 1, \cdots, N_r$, are uniformly distributed on Γ_s and Γ_r, that is, $x_s = R_s(\cos\theta_s, \sin\theta_s), \theta_s = \frac{2\pi}{N_s}(s-1), s = 1, 2, ..., N_s$, and $x_r = R_r(\cos\theta_r, \sin\theta_r), \theta_r = \frac{2\pi}{N_r}(r-1) + \frac{\pi}{N_r}, r = 1, 2, ..., N_r$, so that $x_r \neq x_s$.

Example 5.1. We consider the imaging of sound soft obstacles including a circle, a peanut, a kite and a rounded-square. The imaging domain is $\Omega = (-3, 3) \times (-3, 3)$ with the sampling mesh 201×201. The probe wave wavenumber $k = 4\pi$, $N_s = N_r = 128$, and $R_s = R_r = 10$.

The imaging results are depicted in Fig. 1 which show clearly that our imaging algorithm can find the shape and the location of the obstacles using phaseless data regardless of the shapes of the obstacles.

Example 5.2. We consider the imaging of a 5-leaf obstacle with impedance condition $\eta = 5$, a partially coated obstacle with $\eta = 5$ in the upper boundary and $\eta = 1$ in the lower boundary, a sound hard, and a penetrable obstacle with $n(x) = 0.25$. The imaging domain is $\Omega = (-3, 3) \times (-3, 3)$ with the sampling grid 201×201. The probe wave wavenumber $k = 4\pi$, $N_s = N_r = 128$, and $R_s = R_r = 10$.

Fig. 2 shows the imaging results which demonstrate clearly that our imaging algorithm works for different types of obstacles without using any a prior information of the physical properties of the obstacles.

Example 5.3. We consider the stability of the imaging function with respect to the additive Gaussian random noises using the phaseless data. We introduce the additive Gaussian noise as follows (see e.g. [4]):

$$|u|_{\text{noise}} = |u| + \nu_{\text{noise}},$$

https://doi.org/10.4208/nmtma.2017.m1617 Published online by Cambridge University Press

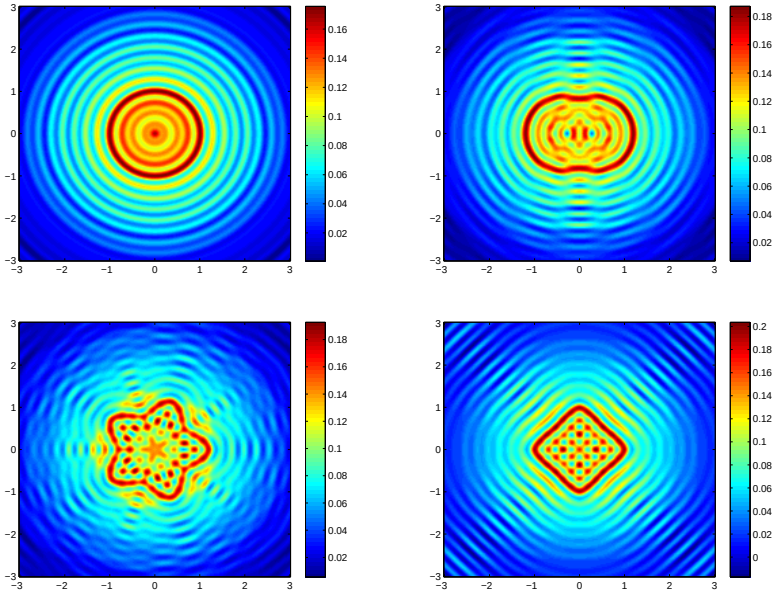


Figure 1: Example 5.1: Imaging results by RTM imaging function (2.4) with phaseless data. Top row: circle (left) and peanut (right); Bottom row: 5-leaf (left) and diamond (right).

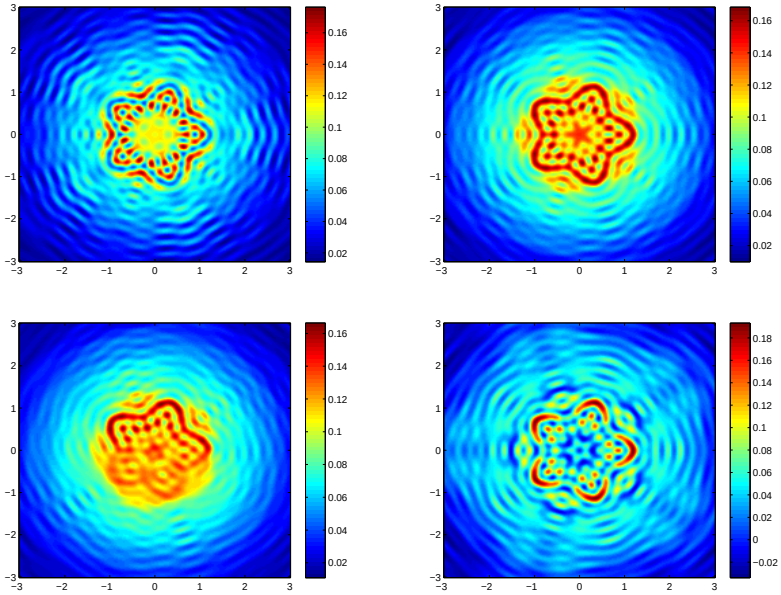
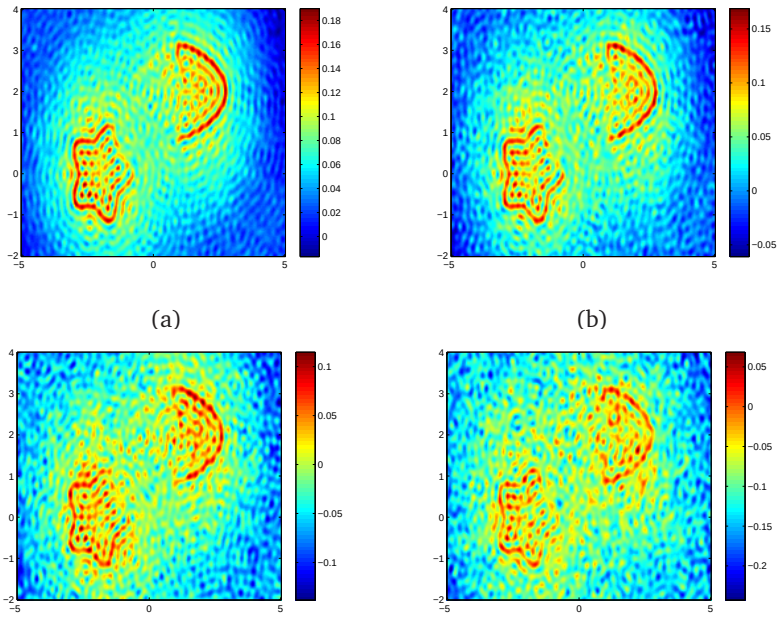


Figure 2: Example 5.2: In the top row, a sound hard 5-leaf obstacle (left) and a non-penetrable obstacle with the impedance $\eta = 5$ (right). In the bottom row, a partially coated obstacle with $\eta = 5$ on the upper boundary and $\eta = 1$ on the lower boundary (left) and a penetrable obstacle with $n(x) = 1/4$ (right).

https://doi.org/10.4208/nmtma.2017.m1617 Published online by Cambridge University Press



(a) (b)

(c) (d)

Figure 3: Example 5.3: The imaging results using single frequency data added with additive Gaussian noise $\mu = 10\%, 20\%, 30\%, 40\%$ from (a) to (d), respectively. The probe wavelength is $\lambda = 0.5$ and the sampling number is $N_s = N_r = 256$.

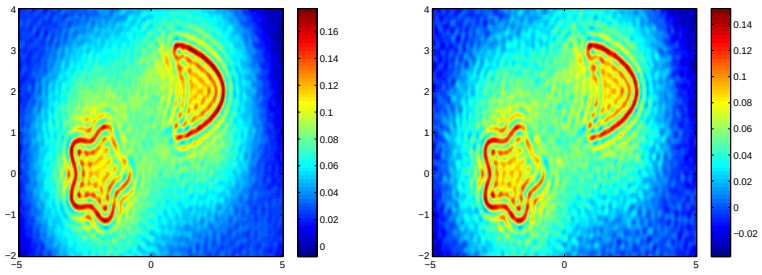
Table 1: Example 5.3: The noise level in the case of single frequency data (left) and multi-frequency data (right).

μ	σ	$\|u\|_{\ell^2}$	$\|\nu_{\text{noise}}\|_{\ell^2}$	μ	σ	$\|u_s\|_{\ell^2}$	$\|\nu_{\text{noise}}\|_{\ell^2}$
0.1	0.003004	0.013017	0.003007	0.1	0.002859	0.013054	0.002863
0.2	0.006009	0.013017	0.005996	0.2	0.005717	0.013054	0.005708
0.3	0.009013	0.013017	0.008964	0.3	0.008576	0.013054	0.008572
0.4	0.012018	0.013017	0.012008	0.4	0.011435	0.013054	0.011424

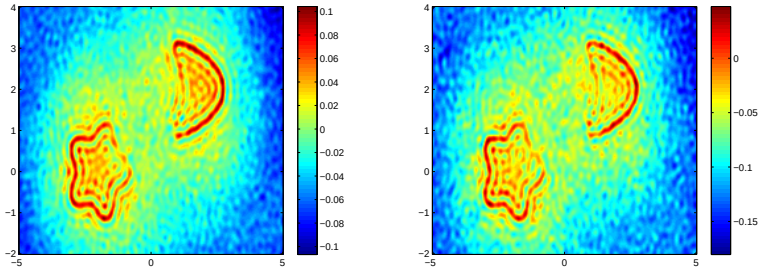
where $|u|$ is the synthesized phaseless total field and ν_{noise} is the Gaussian noise with mean zero and standard deviation μ times the maximum of the data $|u|$, i.e. $\nu_{\text{noise}} = \mu \max |u| \varepsilon$, and $\varepsilon \sim \mathcal{N}(0, 1)$.

For the fixed probe wavenumber $k = 4\pi$, we choose one kite and one 5-leaf in our test. The search domain is $\Omega = (-5, 5) \times (-2, 4)$ with a sampling 201×201 mesh. We set $R_s = 10, R_r = 20$, and $N_s = N_r = 256$. Fig. 3 shows the imaging results for the noise level $\mu = 10\%, 20\%, 30\%, 40\%$ in the single frequency data, respectively. The imaging results can be improved by superposing the multi-frequency imaging result as shown in Fig. 4. The left table in Table 1 shows the noise level, where $\sigma = \mu \max_{x_r, x_s} |u(x_s, x_r)|$,

https://doi.org/10.4208/nmtma.2017.m1617 Published online by Cambridge University Press



(a) (b)



(c) (d)

Figure 4: Example 5.3: The imaging results using multi-frequency data added with additive Gaussian noise $\mu = 10\%, 20\%, 30\%, 40\%$ from (a) to (d), respectively. The probe wavelengths are given by $\lambda = 1/1.8, 1/1.9, 1/2.0, 1/2.1, 1/2.2$ and the sampling number is $N_s = N_r = 256$.

and

$$\|u\|_{\ell^2}^2 = \frac{1}{N_s N_r} \sum_{s,r=1}^{N_s,N_r} |u(x_s, x_r)|^2, \quad \|\nu_{\text{noise}}\|_{\ell^2}^2 = \frac{1}{N_s N_r} \sum_{s,r=1}^{N_s,N_r} |\nu_{\text{noise}}(x_s, x_r)|^2.$$

Acknowledgments This work is supported by National Basic Research Project under the grant 2011CB309700 and China NSF under the grants 11021101 and 11321061.

References

[1] H. Ammari, Y. T. Chow, and J. Zou, *Phased and phaseless domain reconstruction in inverse scattering problem via scattering coefficients*, arXiv: 1510.03999.

[2] G. Bao, P. Li, and J. Lv, *Numerical solution of an inverse diffraction grating problem from phaseless data* , J. Opt. Soc. Am. A, 30 (2013), pp. 293-299.

[3] N. Bleistein, J. Cohen, and J. Stockwell, *Mathematics of Multidimensional Seismic Imaging, Migration, and Inversion*, Springer, 2001.

[4] J. Chen, Z. Chen, and G. Huang, *Reverse time migration for extended obstacles: acoustic waves*, Inverse Problems, 29 (2013), 085005 (17pp).

https://doi.org/10.4208/nmtma.2017.m1617 Published online by Cambridge University Press

[5] J. Chen, Z. Chen, and G. Huang, *Reverse time migration for extended obstacles: electromagnetic waves*, Inverse Problems, 29 (2013), 085006 (17pp).
[6] Z. Chen and G. Huang, *Reverse time migration for extended obstacles: elastic waves*, Science in China Series A: Mathematics (in Chinese), 45 (2015), pp. 1103-1114.
[7] Z. Chen and G. Huang, *Reverse time migration for reconstructing extended obstacles in the half space*, Inverse Problems, 31 (2015), 055007 (19pp).
[8] S. N. Chandler-Wilde, I. G. Graham, S. Langdon, and M. Lindner, *Condition number estimates for combined potential boundary integral operators in acoustic scattering*, J. Integral Equa. Appli., 21 (2009), pp. 229-279.
[9] F. Cakoni, D. Colton, and P. Monk, *The direct and inverse scattering problems for partially coated obstacles* , Inverse Problems, 17 (2001), pp. 1997-2015.
[10] D. Colton and R. Kress, *Inverse Acoustic and Electromagnetic Scattering Problems*, Springer, 1998.
[11] A. J. Devaney, *Structure determination from intensity measurements in scattering experiments*, Physical Review Letters, 62 (1989), pp. 2385-2388.
[12] M. D'Urso, K. Belkebir, L. Crocco, T. Isernia, and A. Litman, *Phaseless imaging with experimental data: facts and challenges,* J. Opt. Soc. Am. A, 25 (2008), pp. 271-281.
[13] G. Franceschini, M. Donelli, R. Azaro, A. and Massa, *Inversion of phaseless total field data using a two-step strategy based on the iterative multiscaling approach*, IEEE Trans. Geosci. Remote Sens., 44 (2006), pp. 3527-3539.
[14] L. Grafakos, *Classical and Modern Fourier Analysis*, Pearson, 2004.
[15] L. Hörmander, *The Analysis of Linear Partial Differential Operators, I*, Springer, 1983.
[16] O. Ivanyshyn and R. Kress, *Identification of sound-soft 3D obstacles from phaseless data*, Inverse Problem and Imaing, 4 (2010), pp. 131-149.
[17] O. Ivanyshyn and R. Kress, *Inverse scattering for surface impedance from phase-less far field data*, Journal of Computational Physics, 230 (2001), pp. 3443-3452.
[18] M. V. Klibanov, *Phaseless inverse scattering problems in threes dimensions*, SIAM J. Appl. Math., 74 (2014), pp. 392-410.
[19] M. V. Klibanov, L. H. Nguyen, and K. Pan, *Nanostructures imaging via numerical solution of a 3-d inverse scattering problem without the phase information*, arXiv: 1404.1183.
[20] M. V. Klibanov and V. G. Romanov, *Explicit formula for the solution of the phaseless inverse scattering problem of imaging of nano structures*, Journal of Inverse and Ill-Posed Problems, (23) 2015, pp. 187-193.
[21] R. Kress, *Integral equation methods in inverse acoustic and electromagnetic scattering* In: Boundary Integral Formulations for Inverse Analysis (Ingham and Wrobel, eds) Computational Mechanics Publications Southampton, 1997, pp. 67-92.
[22] R. Kress and W. Rundell, *Inverse obstacle scattering with modulus of the far field pattern as data* . H. W. Engl et al. (eds.), Inverse Problems in Medical Imaging and Nondestructive Testing, Springer, 1997
[23] R. Leis, *Initial Boundary Value Problems in Mathematical Physics*, B.G. Teubner, 1986
[24] L. Li , H. Zheng, and F. Li, *Two-diensional constant source inversion method with phaseless data: TM case*, IEEE Trans. on Geoscience and remount sensing, 47 (2009), pp. 1719-1736.
[25] A. Litman and K. Belkebir, *Two-dimensional inverse profiling problem using phaseless data*, J. Opt. Soc. Am. A, 23 (2006), pp. 2737-2746.
[26] W. McLean, *Strongly Elliptic Systems and Boundary Integral Equations*, Cambridge University Press, 2000.
[27] R. B Melrose and E. T. Michael,*Near peak scattering and the corrected Kirchhoff ap-*

https://doi.org/10.4208/nmtma.2017.m1617 Published online by Cambridge University Press

proximation for a convex obstacle, Advances in Mathematics, 55 (1985), pp. 242-315.
[28] P. MONK, *Finite Element Methods for Maxwell's Equations*, Clarendon Press, 2003.
[29] R. G. NOVIKOV, *Explicit formulas and global uniqueness for phaseless inverse scattering in multidimensions*, The Journal of Geometric Analysis, (26) 2016, pp. 346-359.
[30] R. G. NOVIKOV, *Formulas for phase recovering from phaseless scattering data at fixed frequency*, Bulletin des Sciences Mathmétiques, (139) 2015, pp. 923-936.
[31] F. OBERHETTINGER AND L. BADII, *Tables of Laplace Transforms*, Springer-Verlag, 1973
[32] R. POTTHAST, *Point-sources and Multipoles in Inverse Scattering Theory*, Chapman and Hall/CRC, 2001.
[33] N. M. TEMME, *Special Functions : An Introduction to the Classical Functions of Mathematical Physics*, Wiley ,1996.
[34] G. N. WATSON, *A Treatise on the Theory of Bessel Functions*, Cambridge University Press, 1995.
[35] B. ZHANG, *On transmission problems for wave propagation in two locally perturbed half-spaces,* Math. Proc. Camb. Phil. Soc., 115 (1994), pp. 545-558.
[36] W. ZHANG, L. LI, AND F. LI, *Inverse scattering from phaseless data in the free space*, Science in China Series F: Information Sciences, 52 (2009), pp. 1389-1398.

https://doi.org/10.4208/nmtma.2017.m1617 Published online by Cambridge University Press